Hindawi
Advances in Polymer Technology
Volume 2019, Article ID 6491532, 10 pages
https://doi.org/10.1155/2019/6491532

Research Article

The Effect of Grafting Density on the Crystallization Behaviors of Polymer Chains Grafted onto One-Dimensional Nanorod

Tongfan Hao,[1] Yongqiang Ming,[2] Shuihua Zhang,[2] Ding Xu,[2] Zhiping Zhou,[2] and Yijing Nie[2]

[1]*Institute of Green Chemistry and Chemical Technology, School of Chemistry and Chemical Engineering, Jiangsu University, 301 Xuefu Road, Zhenjiang 212013, China*
[2]*Institute of Polymer Materials, School of Materials Science and Engineering, Jiangsu University, 301 Xuefu Road, Zhenjiang 212013, China*

Correspondence should be addressed to Zhiping Zhou; zhouzp@ujs.edu.cn and Yijing Nie; nieyijing@ujs.edu.cn

Received 24 October 2018; Accepted 4 December 2018; Published 3 February 2019

Academic Editor: Lu Shao

The crystallization behaviors of five polymer chain systems grafted on a nanorod and the corresponding effect of grafting density were investigated by dynamic Monte Carlo simulations. The segment density near the interfacial regions, the number of crystallites, and the mean square radius of gyration ($< R_g^2 >$) increase with increasing grafting density, which are beneficial to the enhancement of crystallizability. Meanwhile, the crystalline morphology is greatly influenced by grafting density and polymer-nanorod interaction. For the grafted system with 52 chains, a nanohybrid shish-kebab (NHSK) structure is formed, when the polymer-nanorod interaction (E_b/E_c) is -0.4. For the system with 128 chains, a NHSK structure is formed, when E_b/E_c is -1.0. For the system with 252 chains, NHSK structure cannot be formed. The findings in this work can supply important theoretical reference for the design, preparation, and application of polymer nanocomposites.

1. Introduction

It was previously reported that physical properties of composite materials, such as modulus, tensile strength and conductivity, can be dramatically improved by adding fillers into polymers [1–7]. Aluminium oxide, carbon nanotubes, silica particles, and graphene are the commonly used nanoscale fillers, which can significantly change crystalline morphologies of polymer nanocomposites, thus further leading to the improvements in mechanical properties [8–14]. It should be noted that the interaction between polymers and fillers is important for the crystallization of polymer nanocomposites [15, 16]. In general, if weak polymer-filler interaction exists between polymer and nanofillers, the dispersion of nanofillers and the mechanical properties of polymer nanocomposites will be poor [17]. Conversely, the relatively strong polymer-filler interaction can result in the good dispersion of nanofillers and also the excellent mechanical properties [18]. Thus, nowadays, researchers are trying to graft polymer chains onto fillers to enhance the polymer-filler interaction [19–23]. For instance, Yan et al. grafted polyamide 1010 on carbon nanotube and found that the dispersion of carbon nanotube is greatly improved [24]. Baek et al. prepared poly(phenylene sulfide)-graft-carbon nanotube and found that the electrical conductivity, dispersibility, and even melt-processability are improved [25]. Goh et al. grafted polyethylene on carbon nanotube and discovered that the mechanical properties of the corresponding nanocomposites are improved [26].

Nanofillers in polymer matrix can serve as the nucleating agents for polymer crystallization, which strengthen the nucleation ability [25–28]. Obviously, the crystallization process of grafted polymer systems can be affected because of the grafting points, which limit the motion of chain heads and influence the nucleation ability. Jana et al. [23] and Zhou et al. [29] explored the crystallization process of poly(ε-caprolactone)-grafted-carbon nanotubes. They both observed that carbon nanotubes cause the heterogeneous

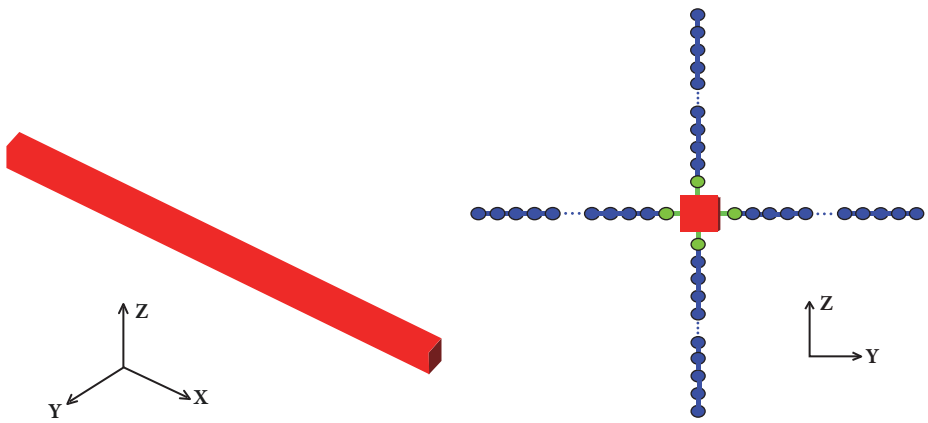

FIGURE 1: (a) Scheme of one-dimensional nanorod with the long axis along the X-axis. (b) The sketch map of four typical polymer chains regularly grafted on four surfaces of the nanorod (this picture was viewed along the X-axis direction). The red parts represent the one-dimensional nanorod, the green sphere represents the segments grafted directly on nanorod, and the blue sphere represents the rest polymer segments.

nucleation of grafted polymer chains. Previously, we investigated the crystallization process of polymer chains graft on two-dimensional filler and observed that the heterogeneous nucleation does not happen with high grafting density under no polymer-filler interaction because of the crowding effect of grafted chains [30]. Moreover, some groups observed that the dimension of fillers seriously affects the crystalline morphology of polymers. For instance, Li et al. observed the appearance of the nanohybrid shish-kebab (NHSK) structure in experiments [31]. Zhou et al. studied the crystallization process of poly(ε-caprolactone)-graft-carbon nanotube but observed that no NHSK structure is formed [29].

In short, the presence of polymer chains grafted on nanofillers can dramatically change the crystallization behaviors of the corresponding polymers, resulting in the remarkable reinforcement effect. As a matter of fact, establishing the relationship between microscopic structures and macroscopic physical properties has always been one of the core tasks in the field of materials science. Thus, in order to prepare the high-performance polymer nanocomposites or effectively regulate physical properties of polymer nanocomposites, the microscopic mechanism of the crystallization of grafted polymers must be first revealed. However, up to now, few experimental studies on the microscopic mechanism of crystallization process for grafted polymers have been reported.

Luckily, computer simulations can supplement the shortcomings of experimental and theoretical work in the investigation of crystallization process for grafted polymers, which can be further used to solve many basic problems raised in the field of polymer materials and also the important technical problems related to the processing of new polymer materials [32–36]. Many groups studied the crystallization behaviors of polymer systems by simulations [37–39]. In this work, we further explored the microscopic mechanism of crystallization process of polymers grafted on one-dimensional nanorod and investigated the effect of grafting density and polymer-nanorod interaction on the corresponding crystallization behaviors.

2. Simulation Details

Monte Carlo simulations [30, 32–36, 40–43] were employed to investigate the crystallization behaviors of grafted polymer systems. It should be noted that dynamic Monte Carlo simulation is a proven method for studying polymer crystallization. Hu et al. have used Monte Carlo simulations to study the different topics in crystallization behaviors of polymers, such as strain- or shear-induced polymer crystallization [40, 41], copolymer crystallization [44, 45], and chain-folding process in polymer crystallization [46]. Previously, our group also applied Monte Carlo simulations to uncover the microscopic mechanisms of crystallization behaviors in polymers [47–49]. A box with 64^3 cubic lattice sites was constructed, and a one-dimensional nanorod with the length, width, and thickness being respective 64, 2 and 2 lattice sites was placed in the middle of the box, for which its long axis is along the X-axis, as exhibited in Figure 1(a). Then, polymer chains with 31 segments were grafted on the four lateral surfaces. Figure 1(b) shows a cross-section of the nanorod perpendicular to the X-axis. It can be seen that four typical grafted chains were grafted on the four lateral surfaces, and the green spheres represented the monomer units grafted directly on the nanorod. In order to explore the influence of grafting density on crystallization process, simulations were carried out for the systems with 52, 64, 84, 128, and 252 grafted polymer chains, respectively. Correspondingly, the grafted densities for the five systems are 0.10, 0.12, 0.16, 0.25, and 0.49. Figure 2 describes the position distributions of grafting points for the five systems with 52(a), 64(b), 84(c), 128(d), and 252(e) grafted polymer chains, respectively. For simplicity, only parts of the one-dimensional nanorod were drawn in Figure 2, and the dashed area represented the rest. During the simulation

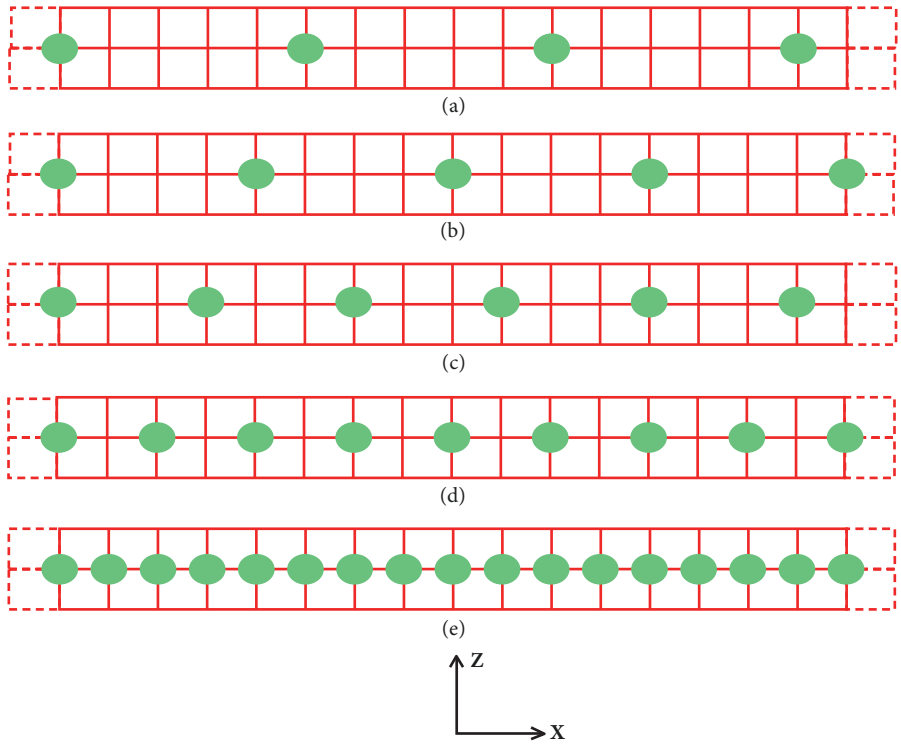

Figure 2: Distributions of the grafting points of the systems containing chains numbers of 52(a), 64(b), 84(c), 128(d), and 252(e), respectively, in the surfaces of the nanorod. The green dot represents the grafted point. The dashed areas on both sides of the rectangles denote the rest parts of the nanorod.

process, one lattice can be occupied by only one segment or one lattice site of the nanorod. A bond connects by two nearby segments, which was oriented along lattice axes or diagonals. Accordingly, the coordination number of one segment site is twenty-six. The polymer chains can move on the basis of a microrelaxation model [35, 36]. In other words, one segment can jump from one lattice to an adjacent vacancy site or slide along the polymer chains. In addition, the segments that were directly grafted on the nanorod were not allowed to move during simulations. Furthermore, periodic boundary conditions were adopted.

The conventional metropolis sampling algorithm was employed in each step of microrelaxation with the potential energy penalty

$$\Delta E = \Delta c \cdot E_c + \Delta p \cdot E_p + \Delta b \cdot E_b \quad (1)$$

E_c is the potential energy change owing to one noncollinear connection of continuous bonds along the chains, which can reflect the pliability of chains, E_p is the interaction energy parameter between two neighboring bonds, which represents the increase in energy caused by the nonparallel arrangements of two neighboring bonds [50, 51], E_b is the interfacial interaction energy between the nanorod and the nearest-neighbor segments [44], Δc and Δp are the numbers of changes of the corresponding noncollinear conformations and nonparallel arrangements of the neighboring bonds before and after sampling in simulations, and Δb is the net change of the nearest-neighbor segment-nanorod pairs. E_p/E_c was set to 1 [32, 33], and kT/E_c was denoted as the simulation temperature, which was further written as $T*$ in following sections. The ratio of polymer-nanorod interaction potential to noncollinear potential (E_b/E_c) was set as 0, -0.1, -0.2, -0.3, -0.4, and -1.0 to explore the influences of polymer-nanorod interactions on the crystallization process of the systems.

The initial polymer chains were relaxed for 10^6 Monte Carlo (MC) cycles to obtain equilibrium amorphous state at an extremely high temperature. Here, one MC cycle denotes the step that all the monomers have one chance to move. As shown in Figure 3, after relaxation the polymer chains have evolved into the random coil state. Subsequently, the random coils were quenched into a simulation temperature $T* = 2.3$.

3. Results and Discussion

The influence of grafting density on the crystallization behaviors of grafted polymer systems without polymer-nanorod interaction was first studied. Figure 4 reveals the evolutions of crystallinity of five systems with different grafting densities during isothermal crystallization process. The definition of crystallinity is the proportion of crystalline bonds (the bonds have more than five parallel neighbors) in all bonds. As shown in Figure 4, after the nucleation induction period (during which the corresponding crystallinity is nearly zero), the values of crystallinity rise immediately and then tend to be stable. In addition, the systems with higher grafting densities have the higher final crystallinity. For the grafted

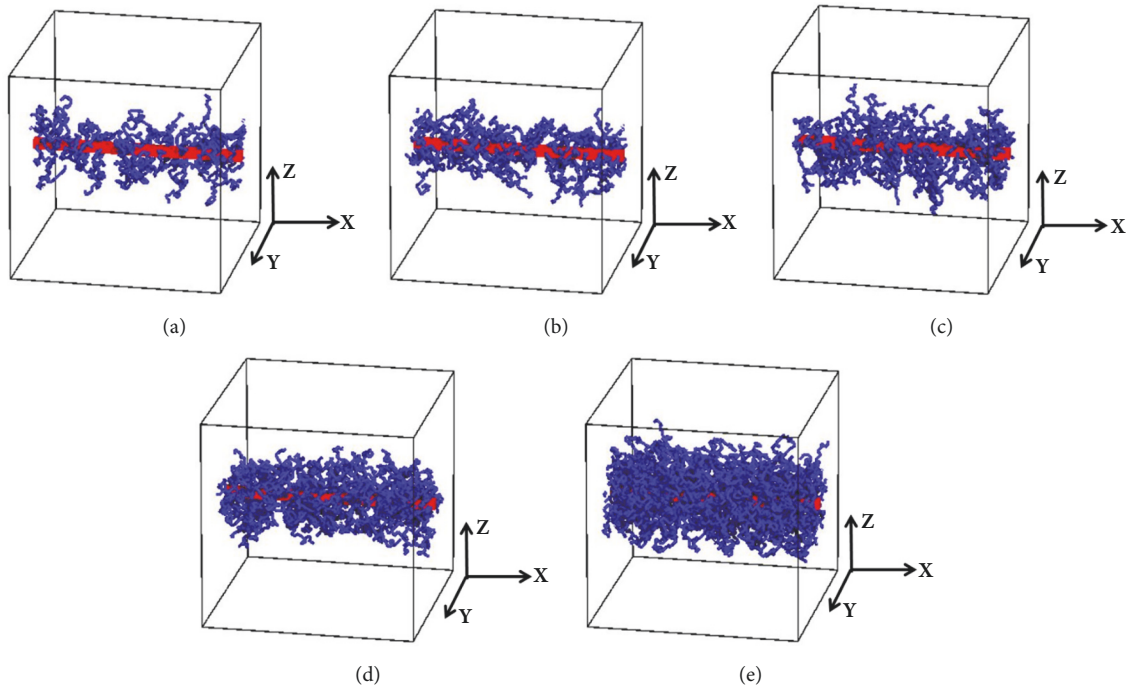

Figure 3: Relaxed polymer systems with 52(a), 64(b), 84(c), 128(d), and 252(e) polymer chains. Blue cylinders denote the polymer chains, and red parts represent the nanorod.

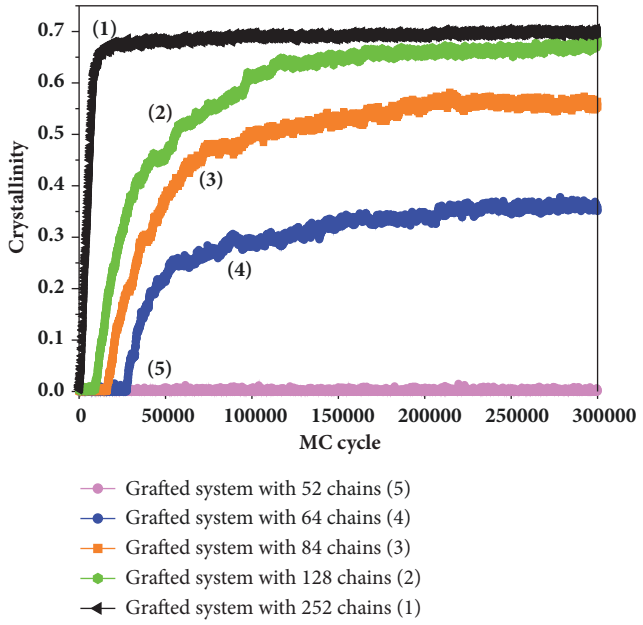

Figure 4: Evolutions of crystallinity for five systems with different grafting densities during isothermal crystallization process, respectively.

system with 52 polymer chains, the crystallinity is almost zero, indicating that crystallization did not occur in this system. It also can be clearly seen that, with increasing grafting density, the nucleation induction period of the grafted polymer system becomes shorter. Zhou et al. prepared poly(ε-caprolactone)-graft-carbon nanotubes and observed that larger nucleation effect exists in the polymers with higher grafting densities [50]. Moreover, the higher grafting density leads to higher final crystallinity for the grafted systems [50]. These conclusions are in accordance with our simulation results. The increase of grafting density can cause the increase of the number of segments. Then, in higher grafting density systems, more crystal nuclei can appear during crystal nucleation, and more segments can take part in the subsequent process of crystal growth, resulting in higher final crystallinity. In the following sections, we focus on the microscopic structure changes of polymer chains during crystallization process for different grafted systems.

The density of segments in interfacial regions can affect polymer crystallization process. Here, the interfacial regions are treated as the first layers next to the nanorod, and the definition of segment density near the surface regions is the ratio of the segment number near the surface regions to the total number of lattice sites near the surface layers. For the blend system of ungrafted polymers and nanorod, the nanorod may limit the conformations of polymer chains near the nanorod surface, causing the conformational entropy reduction. As a result, the segments in the vicinity of the filler surface will be inclined to move towards the exterior zone, leading to the reduction of segment density in the interfacial regions. However, the emergence of this situation can be avoided in the grafted systems. The segment motions of the grafted chains are forcibly restrained by the grafting points, which prevent the grafted chains moving away from the filler surface. Figure 5 shows the segment density near the surface regions of the systems with 52, 64, 84, 128,

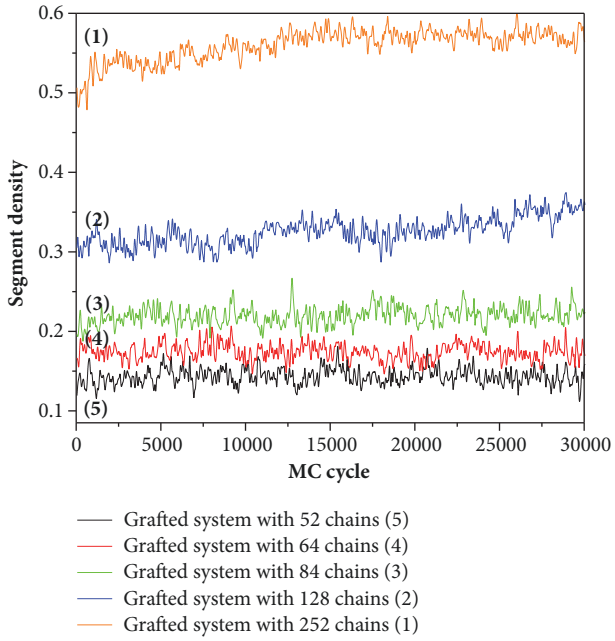

FIGURE 5: Segment density near the nanorod for the grafted polymer systems with 52, 64, 84, 128, and 252 polymer chains, respectively.

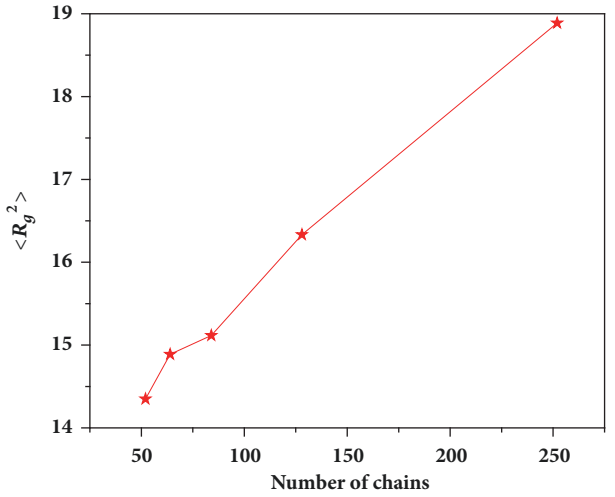

FIGURE 6: $< R_g^2 >$ for the relaxed grafted systems before the crystallization process with 52, 64, 84, 128, and 252 polymer chains, respectively.

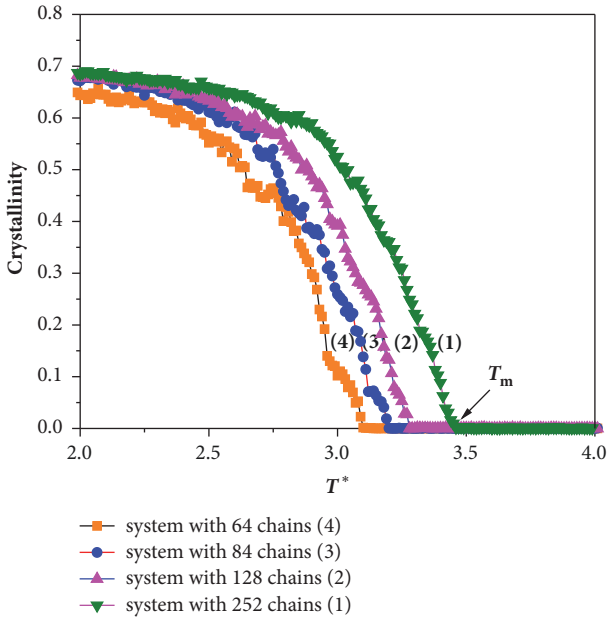

FIGURE 7: Evolutions of crystallinity for the grafted polymer systems with 64, 84, 128, and 252 polymer chains during heating processes, respectively.

and 252 polymer chains, respectively. The segment density increases with increasing chain numbers. In general, the systems with higher segment density usually have higher degree of supercooling and higher melting points. Then, the critical free energy barrier of nucleation is lower [51]. In other words, the ability of nucleation for the systems with higher chain numbers can be enhanced, leading to the shorter nucleation periods, as shown in Figure 4. Similar phenomena were also observed in experiments for the polymers grafted on graphene [52] and carbon nanotubes [21].

Chain conformation can also influence polymer crystal nucleation process in the light of the classic crystal nucleation theory [51, 53]. The existence of grafting points induces the conformation changes of grafted polymer chains. The parameter, mean square radius of gyration ($< R_g^2 >$), can describe the conformations of polymer chains. Figure 6 shows $< R_g^2 >$ of the five relaxed systems before the crystallization process, respectively. Although the length of the polymer chains is identical, the $< R_g^2 >$ still increases with increasing grafting density, implying that the chain conformations are more extended with higher grafted density owing to the stronger crowded effect. Xu et al. studied poly(ε-caprolactone)-g-carbon nanotube with high grafting density and indeed found that grafted polymer chains are overcrowding and highly extended [50]. The crowding effect leads to the loss of conformational entropy and the increase of melting points. For the sake of uncover the influence of grafting density on the melting point, the evolutions of crystallinity for the grafted polymer systems with 64, 84, 128, and 252 polymer chains during heating processes were shown in Figure 7. In order to get the melting temperature, the equilibrium melts of the four grafted systems were cooled with the cooling rate of 0.01 unit of $T*$ per 500 MC cycles from $T* = 5.0$ to 1.0. After that, the systems were heated from $T* = 1.0$ to 5.0. In Figure 7, the melting temperature (T_m) is the temperature when the crystallinity is zero. It is shown that the melting temperatures increase with the increase of grafted density. In brief, the increase of the grafting density causes the significant improvement in melting temperatures, demonstrating that the thermodynamic effect occupies the dominant position.

Figure 8(a) shows the respective initial crystal morphologies of the systems with 64, 84, 128 and 252 polymer chains,

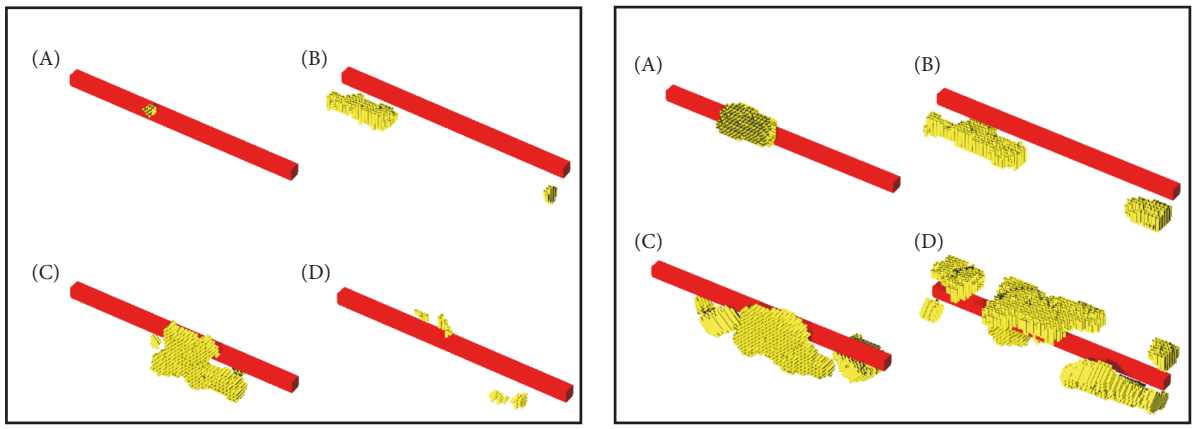

FIGURE 8: Snapshots of small crystallites appearing at the beginning of crystallization (a) and crystalline morphologies at 300000 MC cycles (b) for grafted polymer systems with 64(A), 84(B), 128(C), and 252(D) polymer chains. Yellow cylinders denote the crystalline stems, and red parts denote the nanotubes.

respectively. For the four systems, the initial crystalline stems are inclined to be perpendicular to the long axis of the nanorod. Figure 8(b) demonstrates the corresponding crystalline morphologies at 300000 MC cycles. The initial small crystallites gradually grow into large crystals. It is shown that the crystalline stems in the system with 64 chains (low grafting density) are oriented perpendicular to the long axis of the nanorod. As the grafting density increases, the number of the crystals increases, indicating that more segments can participate in the crystallization. Thus, the systems with higher grafting density have the higher ultimate crystallinity, as shown in Figure 4. Furthermore, the crystals in the systems with high grafting density (128 and 252 chains) exhibit different orientations, but no orientation of crystalline stems along the long axis of the nanorod can be observed. These phenomena can be attributed to the small lateral size of the nanorod and the distributions of the grafting points. As shown in Figure 2, the grafting points are aligned along the long axis of the nanorod, and then the arrangement of segments along the long axis of the nanorod will be hindered owing to the crowding effect. Thus, no crystalline stems oriented along the long axis can be observed in these grafted systems. Furthermore, it should be noted that no NHSK structure can be observed in these grafted systems of different grafting density without polymer-nanorod interaction. In experiment of carbon nanotubes grafted PCL, Xu et al. observed the formation of short rod crystal structures after crystallization. This result is consistent with our current finding (no NHSK structure is found) [50]. Previously, we studied the crystallization process of chains grafted onto a substrate [30]. The crystalline morphology was greatly affected by the change of grafting density. The orientation of the crystalline stems is changed from parallel orientation to the substrate to perpendicular to it, as the grafting density increases [30].

For the polymer/nanorod blends, some groups reported that carbon nanotube can cause the formation of the NHSK structures in experiments [31, 54, 55]. By using computer simulations, Hu et al. detected that an aligned chain can lead to the formation of kebabs [45]. For the polymer-nanorod grafted systems, we further studied the effect of grafting density and polymer-nanorod interactions on crystalline morphology of grafted polymers. From Figure 8(b) we concluded that the crystalline stems oriented along the long axis of the nanorod cannot form, when the interaction between polymer and nanorod is not taken into account. Furthermore, to uncover the influence of the polymer-nanorod interaction, the crystalline morphologies at 300000 MC cycles for three grafted polymer systems containing 52, 128, and 252 chains with the specified polymer-nanorod interaction were shown in Figure 9. For the grafted polymer system with 52 chains (Figure 9(a)), crystallization does not take place, when no interfacial interaction exists (E_b/E_c = 0). Crystallites appear in the systems with lager interfacial interactions (E_b/E_c = -0.1, -0.2, -0.3, -0.4, and -1.0), indicating that the improvement of the polymer-nanorod interaction is beneficial to the crystallization of the grafted polymers. In addition, increasing the polymer-nanorod interaction can lead to the changes of the crystalline morphology. When the value of E_b/E_c is -0.2 or -0.3, the crystalline stems in some crystals start to orient along the long axis of the nanorod. When polymer-nanorod interaction was further increased to E_b/E_c =-0.4 and -1.0, all the crystalline stems exhibit uniform orientation along the long axis of the nanorod, and the typical NHSK structure appears.

However, the influence of polymer-nanorod interaction on crystalline morphologies for the systems with 128 chains is somewhat different from that for the systems with 52 chains. As shown in Figure 9(b), the crystalline stems tend to be perpendicular to the long axis of the nanorod, when E_b/E_c is 0. When E_b/E_c = -0.1, -0.2, -0.3, and -0.4 (higher polymer-nanorod interactions), the crystalline stems in some crystals begin to arrange parallel to the long axis of the nanorod. All crystals show uniform orientation along the long axis of the

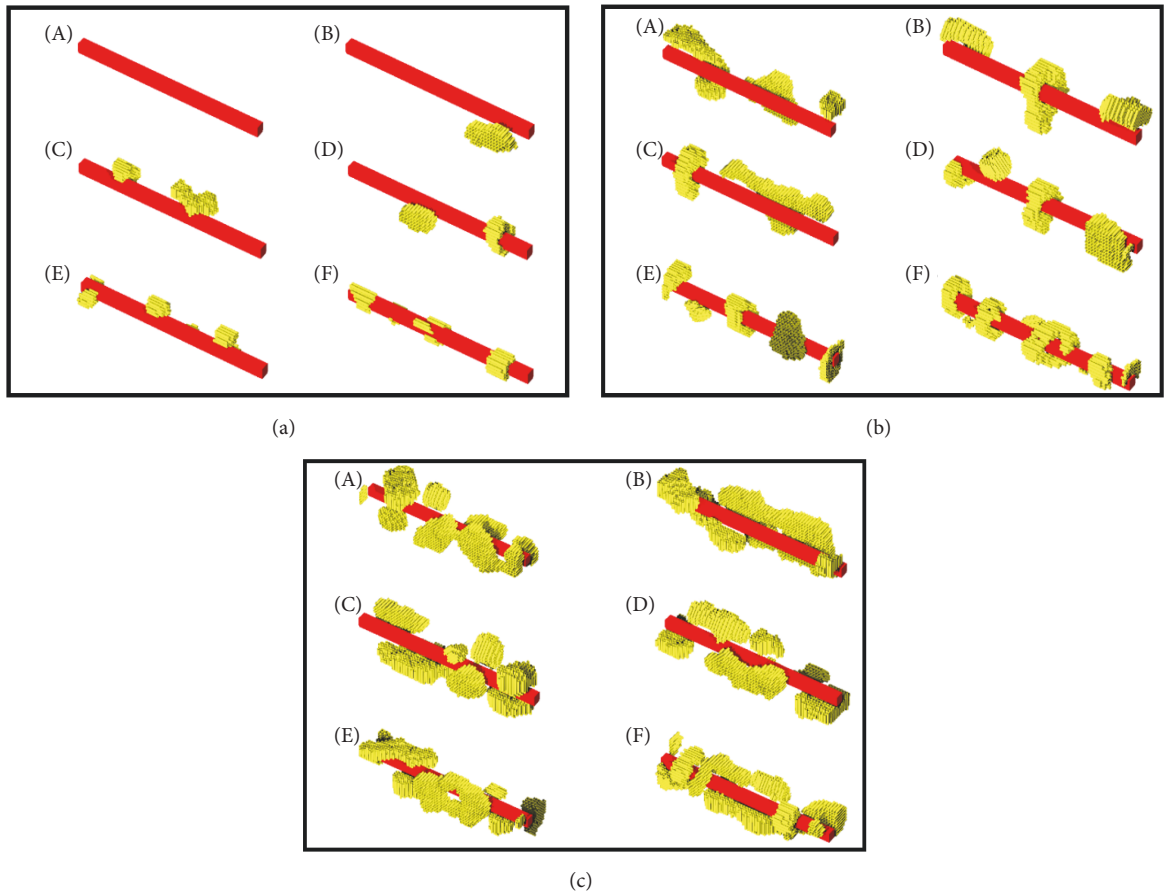

FIGURE 9: The crystalline morphologies on 300000 Monte Carlo cycles of three systems for 52(a), 128(b) and 252(c) polymer chains with the polymer-nanorod interactions of 0 (a)–(c)(A), -0.1 (a)–(c)(B), -0.2 (a)–(c)(C), -0.3 (a)–(c)(D), -0.4 (a)–(c)(E), and -1.0 (a)–(c)(F). Yellow cylinders represent for the crystalline stems and the red parts denote the nanotubes.

nanorod (NHSK structure appears), when the value of E_b/E_c is -1.0. In other words, the NHSK structure in the system with higher grafting density is formed under higher polymer-nanorod interaction.

For the system with 252 polymer chains (Figure 9(c)), no perfect NHSK structure is formed in all the conditions with different polymer-nanorod interactions. This phenomenon can be attributed to the very high grafting density and strong crowding effect. Owing to the strong crowding effect, the chains are forced to "stand" on the nanorod surfaces, the orientation of which tends to be perpendicular to the long axis of the nanorod, as revealed by the largest value of $< R_g^2 >$ of the systems with 252 chains in Figure 6. In experiments, the perfect NHSK structures were observed mainly in polymer/nanorod blend systems. This is the first time that the NHSK structure is observed in the grafted polymer systems. The NHSK structure can only appear with the appropriate grafting density and relatively high polymer-nanorod interaction.

The current simulation results reveal that the crystalline morphology in polymers grafted on one-dimensional nanofiller can be regulated by changing the grafting density and interfacial interaction. Apparently, these systems with different crystalline morphologies should exhibit different physical properties. Thus, we believe that the current findings can provide some guidance for the design and manufacture of new high-performance polymer nanocomposites.

4. Conclusion

The crystallization process of polymer chains grafted onto a nanorod is different from these of the polymer/nanofiller blend system. As the grafting density increases, the nucleation ability and the final crystallinity can be greatly improved. The segment density near the nanorod, the number of crystallites, and the $< R_g^2 >$ of relaxed polymer chains increase with increasing grafting density, which are beneficial to the enhancement of crystallization ability. Meanwhile, the crystalline morphology is also significantly influenced by grafting density and polymer-nanorod interaction. For the grafted system with 52 chains, the NHSK structure appears when the value of E_b/E_c is -0.4. However, the NHSK structure is formed for the grafted system with 128 chains, when the value of E_b/E_c is -1.0. The perfect NHSK structure could not appear in the grafted system of 252 chains under the specified polymer-nanorod interaction owing to the excessively

high grafting density and strong crowding effect. Thus, the formation of NHSK structure requires appropriate grafting density and relatively high polymer-nanorod interaction. This work is helpful for the understanding of the mechanism of crystallization process of grafted systems and can provide some guidance for the design of high-performance polymer composites with the NHSK structure.

Data Availability

The data used to support the findings of this study are included within the article.

Conflicts of Interest

The authors declare that they have no conflicts of interest.

Acknowledgments

This work was supported by the Natural Science Foundation of the Higher Education Institutions of Jiangsu Province (no. 18KJB150009) and the National Natural Science Foundation of China (no. 21404050).

References

[1] P. Jojibabu, G. D. J. Ram, A. P. Deshpande, and S. R. Bakshi, "Effect of carbon nano-filler addition on the degradation of epoxy adhesive joints subjected to hygrothermal aging," *Polymer Degradation and Stability*, vol. 140, pp. 84–94, 2017.

[2] W. Liu, N. Liu, J. Sun et al., "Ionic Conductivity Enhancement of Polymer Electrolytes with Ceramic Nanowire Fillers," *Nano Letters*, vol. 15, no. 4, pp. 2740–2745, 2015.

[3] N. El Miri, F. Aziz, A. Aboulkas, M. El Bouchti, H. Ben Youcef, and M. El Achaby, "Effect of plasticizers on physicochemical properties of cellulose nanocrystals filled alginate bionanocomposite films," *Advances in Polymer Technology*, pp. 1–15, 2018.

[4] J. Chanra, E. Budianto, and B. Soegijono, "Synthesis of polymer hybrid latex poly(methyl methacrylate-co-butyl acrylate) with organo montmorillonite via miniemulsion polymerization method for barrier paper," *Journal of Physics: Conference Series*, vol. 985, p. 012029, 2018.

[5] N. Vicentini, T. Gatti, M. Salerno et al., "Effect of different functionalized carbon nanostructures as fillers on the physical properties of biocompatible poly(l -lactic acid) composites," *Materials Chemistry and Physics*, vol. 214, pp. 265–276, 2018.

[6] J.-Y. Kim, T. Kim, J. W. Suk et al., "Enhanced dielectric performance in polymer composite films with carbon nanotube-reduced graphene oxide hybrid filler," *Small*, vol. 10, no. 16, pp. 3405–3411, 2014.

[7] S. Cheng, X. Chen, Y. G. Hsuan, and C. Y. Li, "Reduced graphene oxide-induced polyethylene crystallization in solution and nanocomposites," *Macromolecules* , vol. 45, no. 2, pp. 993–1000, 2012.

[8] S. Ye, X. Zeng, F. Tan, and Q. Fan, "Research on the tribological performance of Cr2O3 filled with bronze-based PTFE composites," *Journal of Applied Polymer Science*, vol. 131, no. 22, Article ID 41117, 2014.

[9] C. Pagano, R. Surace, V. Bellantone, F. Baldi, and I. Fassi, "Mechanical characterisation and replication quality analysis of micro-injected parts made of carbon nanotube/polyoxymethylene nanocomposites," *Journal of Composite Materials*, vol. 52, no. 5, pp. 645–657, 2018.

[10] E. D. Vogli, O. Turkarslan, S. M. Iconomopoulou, D. Korkmaz, A. Soto Beobide, and G. A. Voyiatzis, "From lab-scale film preparation to up- scale spinning fibre manufacturing of multi-wall carbon nanotube/poly ethylene terephthalate composites," *Journal of Industrial Textiles*, vol. 47, no. 6, pp. 1241–1260, 2018.

[11] S. Farhanian and M. Hatami, "Thermal and morphological aspects of silver decorated halloysite reinforced polypropylene nanocomposites," *Journal of Thermal Analysis and Calorimetry*, vol. 130, no. 3, pp. 2069–2078, 2017.

[12] R. H. Hakim, J. Cailloux, O. O. Santana et al., "PLA/SiO2 composites: Influence of the filler modifications on the morphology, crystallization behavior, and mechanical properties," *Journal of Applied Polymer Science*, vol. 134, no. 40, Article ID 45367, 2017.

[13] E. Tarani, D. G. Papageorgiou, C. Valles et al., "Insights into crystallization and melting of high density polyethylene/graphene nanocomposites studied by fast scanning calorimetry," *Polymer Testing*, vol. 67, pp. 349–358, 2018.

[14] L. Sisti, G. Totaro, M. Vannini, L. Giorgini, S. Ligi, and A. Celli, "Bio-Based PA11/Graphene Nanocomposites Prepared by in Situ Polymerization," *Journal of Nanoscience and Nanotechnology*, vol. 18, no. 2, pp. 1169–1175, 2018.

[15] X. Hu, H. An, Z.-M. Li, Y. Geng, L. Li, and C. Yang, "Origin of carbon nanotubes induced poly(l-lactide) crystallization: Surface induced conformational order," *Macromolecules* , vol. 42, no. 8, pp. 3215–3218, 2009.

[16] N. Patil, L. Balzano, G. Portale, and S. Rastogi, "A study on the chain-particle interaction and aspect ratio of nanoparticles on structure development of a linear polymer," *Macromolecules* , vol. 43, no. 16, pp. 6749–6759, 2010.

[17] R. Czerw, Z. Guo, P. M. Ajayan, Y.-P. Sun, and D. L. Carroll, "Organization of Polymers onto Carbon Nanotubes: A Route to Nanoscale Assembly," *Nano Letters*, vol. 1, no. 8, pp. 423–427, 2001.

[18] L. Karásek and M. Sumita, "Characterization of dispersion state of filler and polymer-filler interactions in rubber-carbon black composites," *Journal of Materials Science*, vol. 31, no. 2, pp. 281–289, 1996.

[19] H. J. Salavagione, G. Martínez, and G. Ellis, "Recent advances in the covalent modification of graphene with polymers," *Macromolecular Rapid Communications*, vol. 32, no. 22, pp. 1771–1789, 2011.

[20] L. Kan, Z. Xu, and C. Gao, "General avenue to individually dispersed graphene oxide-based two-dimensional molecular brushes by free radical polymerization," *Macromolecules* , vol. 44, no. 3, pp. 444–452, 2011.

[21] B. Zhou, Z.-Z. Tong, J. Huang, J.-T. Xu, and Z.-Q. Fan, "Synthesis and thermal behavior of poly(ε-caprolactone) grafted on multi-walled carbon nanotubes with high grafting degrees," *Materials Chemistry and Physics*, vol. 137, no. 3, pp. 1053–1061, 2013.

[22] G.-X. Chen, H.-S. Kim, B. H. Park, and J.-S. Yoon, "Controlled functionalization of multiwalled carbon nanotubes with various molecular-weight poly(L-lactic acid)," *The Journal of Physical Chemistry B*, vol. 109, no. 47, pp. 22237–22243, 2005.

[23] R. N. Jana and J. W. Cho, "Thermal stability, crystallization behavior, and phase morphology of poly(ε-caprolactone)diol-grafted-multiwalled carbon nanotubes," *Journal of Applied Polymer Science*, vol. 110, no. 3, pp. 1550–1558, 2008.

[24] H. Zeng, C. Gao, Y. Wang et al., "In situ polymerization approach to multiwalled carbon nanotubes-reinforced nylon

1010 composites: Mechanical properties and crystallization behavior," *Polymer Journal*, vol. 47, no. 1, pp. 113–122, 2006.

[25] I.-Y. Jeon, H.-J. Lee, Y. S. Choi, L.-S. Tan, and J.-B. Baek, "Semimetallic transport in nanocomposites derived from grafting of linear and hyperbranched poly(phenylene sulfide)s onto the surface of functionalized multi-walled carbon nanotubes," *Macromolecules* , vol. 41, no. 20, pp. 7423–7432, 2008.

[26] B.-X. Yang, K. P. Pramoda, G. Q. Xu, and S. H. Goh, "Mechanical reinforcement of polyethylene using polyethylene-grafted multiwalled carbon nanotubes," *Advanced Functional Materials*, vol. 17, no. 13, pp. 2062–2069, 2007.

[27] N. Ning, S. Fu, W. Zhang et al., "Realizing the enhancement of interfacial interaction in semicrystalline polymer/filler composites via interfacial crystallization," *Progress in Polymer Science*, vol. 37, no. 10, pp. 1425–1455, 2012.

[28] J.-Z. Xu, G.-J. Zhong, B. S. Hsiao, Q. Fu, and Z.-M. Li, "Low-dimensional carbonaceous nanofiller induced polymer crystallization," *Progress in Polymer Science*, vol. 39, no. 3, pp. 555–593, 2014.

[29] B. Zhou, W.-N. He, X.-Y. Jiang, Z.-Z. Tong, J.-T. Xu, and Z.-Q. Fan, "Effect of molecular weight on isothermal crystallization kinetics of multi-walled carbon nanotubes-graft-poly(ε-caprolactone)," *Composites Science and Technology*, vol. 93, pp. 23–29, 2014.

[30] T. Hao, Z. Zhou, Y. Nie, L. Zhu, Y. Wei, and S. Li, "Molecular simulations of crystallization behaviors of polymers grafted on two-dimensional filler," *Polymer (United Kingdom)*, vol. 100, pp. 10–18, 2016.

[31] L. Li, C. Y. Li, and C. Ni, "Polymer crystallization-driven, periodic patterning on carbon nanotubes," *Journal of the American Chemical Society*, vol. 128, no. 5, pp. 1692–1699, 2006.

[32] Y. Nie, T. Hao, Z. Gu et al., "Relaxation and Crystallization of Oriented Polymer Melts with Anisotropic Filler Networks," *The Journal of Physical Chemistry B*, vol. 121, no. 6, pp. 1426–1437, 2017.

[33] Y. Nie, T. Hao, Y. Wei, and Z. Zhou, "Polymer crystal nucleation with confinement-enhanced orientation dominating the formation of nanohybrid shish-kebabs with multiple shish," *RSC Advances*, vol. 6, no. 56, pp. 50451–50459, 2016.

[34] Y. Ming, Z. Zhou, D. Xu, R. Liu, Y. Nie, and T. Hao, "The effect of molecular weight of polymers grafted in two-dimensional filler on crystallization behaviors studied by dynamic Monte Carlo simulations," *Computational Materials Science*, vol. 155, pp. 144–150, 2018.

[35] R. Liu, L. Yang, X. Qiu et al., "One-dimensional nanofiller induced crystallization in random copolymers studied by dynamic Monte Carlo simulations," *Molecular Simulation*, pp. 1–9, 2018.

[36] T. Hao, Z. Zhou, Y. Wang et al., "Segmental dynamics in interfacial region of composite materials," *Monatshefte für Chemie - Chemical Monthly*, vol. 148, no. 7, pp. 1285–1293, 2017.

[37] H. Xiao, C. Luo, D. Yan, and J.-U. Sommer, "Molecular Dynamics Simulation of Crystallization Cyclic Polymer Melts As Compared to Their Linear Counterparts," *Macromolecules* , vol. 50, no. 24, pp. 9796–9806, 2017.

[38] H. Meyer and F. Müller-Plathe, "Formation of chain-bolded structures in supercooled polymer melts examined by MD simulations," *Macromolecules* , vol. 35, no. 4, pp. 1241–1252, 2002.

[39] T. Hao, Z. Zhou, Y. Nie, Y. Wei, Z. Gu, and S. Li, "Effect of the polymer-substrate interactions on crystal nucleation of polymers grafted on a flat solid substrate as studied by molecular simulations," *Polymer (United Kingdom)*, vol. 123, pp. 169–178, 2017.

[40] Y. Nie, H. Gao, M. Yu, Z. Hu, G. Reiter, and W. Hu, "Competition of crystal nucleation to fabricate the oriented semi-crystalline polymers," *Polymer (United Kingdom)*, vol. 54, no. 13, pp. 3402–3407, 2013.

[41] Y. Nie, H. Gao, and W. Hu, "Variable trends of chain-folding in separate stages of strain-induced crystallization of bulk polymers," *Polymer (United Kingdom)*, vol. 55, no. 5, pp. 1267–1272, 2014.

[42] W. B. Hu and D. Frenkel, "Polymer Crystallization Driven by Anisotropic Interactions," *Advances in Polymer Science*, vol. 191, pp. 1–35, 2005.

[43] W. Hu, D. Frenkel, and V. B. F. Mathot, "Simulation of Shish-Kebab crystallite induced by a single prealigned macromolecule," *Macromolecules* , vol. 35, no. 19, pp. 7172–7174, 2002.

[44] Y. Nie, H. Gao, Y. Wu, and W. Hu, "Thermodynamics of strain-induced crystallization of random copolymers," *Soft Matter*, vol. 10, no. 2, pp. 343–347, 2014.

[45] H. Gao, M. Vadlamudi, R. G. Alamo, and W. Hu, "Monte carlo simulations of strong memory effect of crystallization in random copolymers," *Macromolecules* , vol. 46, no. 16, pp. 6498–6506, 2013.

[46] X. Jiang, G. Reiter, and W. Hu, "How Chain-Folding Crystal Growth Determines the Thermodynamic Stability of Polymer Crystals," *The Journal of Physical Chemistry B*, vol. 120, no. 3, pp. 566–571, 2016.

[47] Y. Nie, Z. Gu, Q. Zhou et al., "Controllability of Polymer Crystal Orientation Using Heterogeneous Nucleation of Deformed Polymer Loops Grafted on Two-Dimensional Nanofiller," *The Journal of Physical Chemistry B*, vol. 121, no. 27, pp. 6685–6690, 2017.

[48] Z. Gu, R. Yang, J. Yang et al., "Dynamic Monte Carlo simulations of effects of nanoparticle on polymer crystallization in polymer solutions," *Computational Materials Science*, vol. 147, pp. 217–226, 2018.

[49] H. Wu, X. Qiu, Y. Zhang et al., "Formation mechanism of reverse kebab structure inside hollow nanotubes studied by molecular simulations," *Computational Materials Science*, vol. 153, pp. 348–355, 2018.

[50] B. Zhou, Z.-Z. Tong, J. Huang, J.-T. Xu, and Z.-Q. Fan, "Isothermal crystallization kinetics of multi-walled carbon nanotubes-graft-poly(ε-caprolactone) with high grafting degrees," *CrystEngComm*, vol. 15, no. 38, pp. 7824–7832, 2013.

[51] W. Hu, *Polymer Physics, a Molecular Approach*, Springer, Vienna, Austria, 2013.

[52] T. Mondal, R. Ashkar, P. Butler, A. K. Bhowmick, and R. Krishnamoorti, "Graphene Nanocomposites with High Molecular Weight Poly(ε-caprolactone) Grafts: Controlled Synthesis and Accelerated Crystallization," *ACS Macro Letters*, vol. 5, no. 3, pp. 278–282, 2016.

[53] Y. Nie, G. Huang, L. Qu, X. Wang, G. Weng, and J. Wu, "New insights into thermodynamic description of strain-induced crystallization of peroxide cross-linked natural rubber filled with clay by tube model," *Polymer Journal*, vol. 52, no. 14, pp. 3234–3242, 2011.

[54] L. Chen, Z. Chen, X. Li, W. Huang, X. Li, and X. Liu, "Dynamic imine chemistry assisted reaction induced hetero-epitaxial crystallization: Novel approach towards aromatic polymer/CNT nanohybrid shish-kebabs and related hybrid crystalline structures," *Polymer (United Kingdom)*, vol. 54, no. 7, pp. 1739–1745, 2013.

[55] W. Wang, Z. Huang, E. D. Laird, S. Wang, and C. Y. Li, "Single-walled carbon nanotube nanoring induces polymer crystallization at liquid/liquid interface," *Polymer (United Kingdom)*, vol. 59, pp. 1–9, 2015.